# Nonideal quantum nondemolition measurements

M. J. Holland, M. J. Collett, and D. F. Walls
*Department of Physics, University of Auckland, New Zealand*

M. D. Levenson
*IBM Research Laboratories, San Jose, California*
(Received 21 March 1990)

The process of making a measurement on a quantum-mechanical system introduces quantum noise to that system. A quantum nondemolition measurement scheme seeks to make a measurement of an observable to better than this quantum limit, by feeding all the introduced noise into a conjugate variable to that under consideration. In this paper three quantitative criteria are suggested for the evaluation of nonideal quantum nondemolition measurements. The application of these criteria is illustrated using both a simple beam splitter and the $\chi^3$ interaction in a Raman-active medium.

## I. INTRODUCTION

General principles of quantum nondemolition (QND) measurements have been discussed in the literature by Caves *et al.*,[1] and recently there have been a number of theoretical papers[2–6] proposing schemes for quantum nondemolition of back-action-evading measurements in optics. There have also been somewhat fewer experimental realizations.[7,8] In this paper we wish to define clearly the objectives of such quantum measurements. These objectives may differ depending on the motivation for the measurement. For example, in a transmission line with a series of receivers, the goal may be to tap information from the signal without degrading the signal transmitted to the next receiver. In a system used to measure the magnitude of an external force, the goal of the quantum measurement may be state preparation. That is, an initial measurement prepares the system in a known quantum state. The presence of a perturbing force will be detected by a subsequent measurement on the system.

We shall define a set of criteria for quantum measurements, one or more of which may be desirable in a given experimental situation. As a benchmark to evaluate the effectiveness of any scheme as a QND device, we shall use a beam splitter deflecting part of a signal to a detector.

To illustrate the utility of the criteria we have introduced, we consider two examples of nonideal QND measurements. The first scheme we consider is a near resonant Raman transition. This differs from ideal QND schemes which are based on far-from-resonance transitions. The advantage of a near-resonant transition is that it gives a higher nonlinearity, but the QND character may be degraded by loss and scattering. We evaluate the performance of the system as a QND device for various detunings from the resonant transtion. We are able to find regimes of operation where the Raman system will have an enhanced performance with respect to the beam splitter. Experimental results based on a Raman system will be discussed in a future publication. As a second example of a nonideal QND measurement we consider a beam splitter with a squeezed probe input.

## II. QND CRITERIA

We consider making a good quantum nondemolition measurement of the amplitude quadrature of an optical signal field. If the boson annihilation operator for the signal is $a$, then appropriate definitions for the amplitude quadrature $X_a$ and phase quadrature $X_p$ are given by

$$X_a = a + a^\dagger ,$$
$$X_p = i(a^\dagger - a) . \tag{1}$$

Note that according to Heisenberg's uncertainty principle

$$\Delta X_a \Delta X_p \geq 1 , \tag{2}$$

where $\Delta X_a$ and $\Delta X_p$ are the root-mean-square deviations. A precise measurement of the amplitude quadrature must therefore be at the expense of uncertainty in the phase. A good back-action-evading scheme must be able to feed all the quantum noise induced by the act of measurement into the phase quadrature of the signal leaving the apparatus. In the general scheme we consider here, the amplitude quadrature of the signal interacts in the apparatus with the phase quadrature of the probe field on which a subsequent readout measurement can be made (Fig. 1). If the annihilation operator for the probe field is $b$, then appropriate definitions for the amplitude quadrature $Y_a$ and the phase quadrature $Y_p$ are given by

$$Y_a = b + b^\dagger ,$$
$$Y_p = i(b^\dagger - b) . \tag{3}$$

The interaction must be such that there is a strong correlation of the probe leaving the apparatus to the signal field. In an ideal QND scheme, the input and output quadratures are related by

$$X_a^{\text{out}} = X_a^{\text{in}} ,$$
$$Y_p^{\text{out}} = G X_a^{\text{in}} , \tag{4}$$

where the variable $G$ is known as the QND gain. In a

 

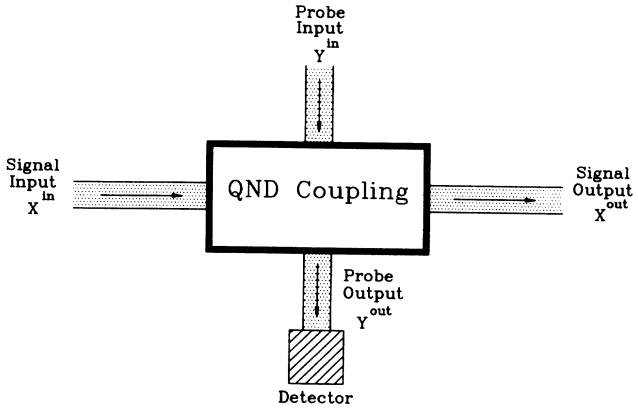


FIG. 1. A schematic quantum nondemolition device. The signal field interacts with the probe field in the apparatus. A subsequent readout measurement of the probe output is then well correlated with either the signal input making a good measurement, or the signal output preparing a well-known state.

system which satisfies this, the amplitude quadrature of the signal is not perturbed at all by the interaction, and the phase quadrature of the output probe is perfectly correlated with the incident signal.

In practice, real QND couplings using nonlinear optical interactions may have additional terms corresponding to quantum fluctuations in the incident probe field and additional scattering processes. There is a requirement for criteria which evaluate the performance of a QND measurement scheme operating in a nonideal regime. We can describe the fluctuating quantum or classical noise in terms of the variances of the two input and two output fields;

$$\begin{aligned} V_{X_a^{in}} &= \langle (X_a^{in})^2 \rangle - \langle X_a^{in} \rangle^2 , \\ V_{Y_p^{in}} &= \langle (Y_p^{in})^2 \rangle - \langle Y_p^{in} \rangle^2 , \\ V_{X_a^{out}} &= \langle (X_a^{out})^2 \rangle - \langle X_a^{out} \rangle^2 , \\ V_{Y_p^{out}} &= \langle (Y_p^{out})^2 \rangle - \langle Y_p^{out} \rangle^2 . \end{aligned} \tag{5}$$

When examining a possible QND scheme there are three criteria to consider.

1. *How good is the scheme as a measurement device?* This is determined by the level of correlation between the probe field measured by a detector and the signal field incident on the apparatus,

$$C^2_{X_a^{in} Y_p^{out}} = \frac{|\langle X_a^{in} Y_p^{out} \rangle - \langle X_a^{in} \rangle \langle Y_p^{out} \rangle|^2}{V_{X_a^{in}} V_{Y_p^{out}}} . \tag{6}$$

For a perfect measurement device, the phase quadrature of the probe output is equal to the amplitude of the signal input multiplied by the QND gain. For this situation, the correlation coefficient is unity.

2. *How much does the scheme degrade the signal field?* The quantity of interest here is the correlation between the signal input field and the signal output field,

$$C^2_{X_a^{in} X_a^{out}} = \frac{|\langle X_a^{in} X_a^{out} \rangle - \langle X_a^{in} \rangle \langle X_a^{out} \rangle|^2}{V_{X_a^{in}} V_{X_a^{out}}} . \tag{7}$$

This is a measure of the QND effect, the ability of a scheme to isolate quantum noise introduced by the measurement process from the observable of interest. For an ideal QND scheme we require this correlation to be unity.

3. *How good is the scheme as a state-preparation device?* If we have a perfect measurement device that does not degrade the signal at all, i.e., we satisfy the two previous requirements exactly, then we must be able to completely predict the state of the signal output. However, once we leave this ideal case, the predictability of the signal output is no longer fully determined by correlations with the signal input. The extreme example is that of a destructive measurement: independently of how well the input is measured, the output is always a vacuum. On the other hand, the correlation between the signal and probe output fields is not a good indicator of the quality of state preparation. Figure 2 shows a situation in which both output fields are well correlated, but a probe measurement does not allow inference of the value of the signal output field to better than the quantum limit. This situation arises when the interaction within the QND medium introduces significant *correlated* noise to both output fields. A better indicator to measure the quality of state preparation for a possible QND scheme is the variance in the signal output given a measured value for the probe field. If the output fields can be described by gaussian probabilities, or the predictor for the signal field given measurement of the probe is linear,

$$E[X_a^{out} | Y_p^{out}] = \alpha + \beta Y_p^{out} , \tag{8}$$

then we can evaluate the performance of a state-

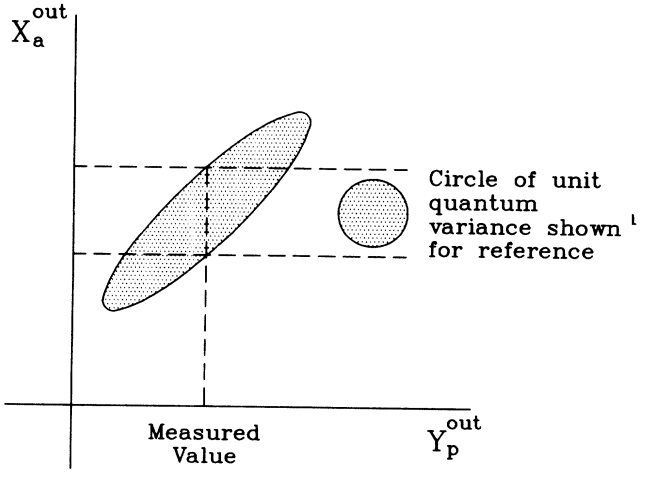


FIG. 2. Good correlation between the signal output and the probe output does not necessarily indicate a good state preparation device. The diagram illustrates a situation in which a value of the probe output has been measured but when mapped onto the error ellipse does not allow inference of the value of the signal to better than the quantum limit.

preparation device by considering

$$C^2_{X_a^{\rm out}Y_p^{\rm out}}=\frac{|\langle X_a^{\rm out}Y_p^{\rm out}\rangle-\langle X_a^{\rm out}\rangle\langle Y_p^{\rm out}\rangle|^2}{V_{X_a^{\rm out}}V_{Y_p^{\rm out}}}\ ,$$
$$V(X_a^{\rm out}|Y_p^{\rm out})=V_{X_a^{\rm out}}(1-C^2_{X_a^{\rm out}Y_p^{\rm out}})\ . \tag{9}$$

A perfect state-preparation device would have zero variance, which occurs for $C^2_{X_a^{\rm out}Y_p^{\rm out}}=1$.

## III. THE BEAM SPLITTER

We consider first a quantum-mechanical beam splitter deflecting part of the incident electromagnetic signal field onto a homodyne detector (Fig. 3). From the point of view of comparison this is an ideal device to analyze. There is obviously little point in constructing complicated cavities containing nonlinear media, or using off-resonance atomic transitions, for example, if these devices cannot improve on this simple scheme.

We would like the beam splitter to measure the amplitude quadrature of the input signal field, report an eigenvalue of this observable, and leave the signal field in the corresponding eigenstate. The phase change on reflection gives coupling between the amplitude quadrature of the signal field and the phase quadrature of the probe. The input quadrature fields can be related to the output quadrature fields using the transformation at the beam splitter,

$$\begin{bmatrix}X_a^{\rm out}\\ Y_p^{\rm out}\end{bmatrix}=\begin{bmatrix}(1-\eta^2)^{1/2} & -\eta\\ \eta & (1-\eta^2)^{1/2}\end{bmatrix}\begin{bmatrix}X_a^{\rm in}\\ Y_p^{\rm in}\end{bmatrix}\ . \tag{10}$$

where $\eta$ is real and represents the mirror amplitude reflectivity, and there is a $\pi/2$ phase change upon reflection.

The first criterion for a good QND measurement scheme is that it must be a good back-action-evading device. In other words, it must be able to isolate the signal field from quantum noise introduced by making the measurement. How well the beam splitter achieves this is represented by the correlation between the input and output signal fields,

$$C^2_{X_a^{\rm in}X_a^{\rm out}}=\frac{(1-\eta^2)V_{X_a^{\rm in}}}{(1-\eta^2)V_{X_a^{\rm in}}+\eta^2V_{Y_p^{\rm in}}}\ , \tag{11}$$

where $V_{X_a^{\rm in}}$ denotes the variance of the signal input and $V_{Y^{p\,\rm in}}$ correspondingly for the probe. These quantities are a measure of the magnitude of quantum or classical noise present in the input fields at the appropriate quadrature phase. For a beam splitter with 50% reflectivity, the correlation between the signal input and output is given by the ratio of the signal noise to the total noise introduced to the system through both input ports.

The second criterion is how well the scheme acts as a measurement device. The readout measurement is made on the probe output field, so the level of correlation between this quantity and the signal field incident on the device determines how well a measurement can be made. The appropriate correlation coefficient is

$$C^2_{X_a^{\rm in}y_p^{\rm out}}=\frac{\eta^2V_{X_a^{\rm in}}}{\eta^2V_{X_a^{\rm in}}+(1-\eta^2)V_{Y_p^{\rm in}}}\ . \tag{12}$$

Again for a 50% beam splitter, the correlation is given by the ratio of the incident signal noise to the total introduced noise.

The third criterion is that the measurement must prepare the output observable in a well-known state. This is given by the variance in the output state after the measurement has been performed. Using

$$C^2_{X_a^{\rm out}Y_p^{\rm out}}=\frac{\eta^2(1-\eta^2)(V_{X_a^{\rm in}}-V_{Y_p^{\rm in}})^2}{[(1-\eta^2)V_{X_a^{\rm in}}+\eta^2V_{Y_p^{\rm in}}][\eta^2V_{X_a^{\rm in}}+(1-\eta^2)V_{Y_p^{\rm in}}]}\ ,$$
$$V_{X_a^{\rm out}}=(1-\eta^2)V_{X_a^{\rm in}}+\eta^2V_{Y_p^{\rm in}}\ , \tag{13}$$

and that the predictor for the beam splitter is linear, the residual variance is given by

$$V(X_a^{\rm out}|Y_p^{\rm out})=V_{X_a^{\rm out}}(1-C^2_{X_a^{\rm out}Y_p^{\rm out}})$$
$$=\frac{V_{X_a^{\rm in}}V_{Y_p^{\rm in}}}{\eta^2V_{X_a^{\rm in}}+(1-\eta^2)V_{Y_p^{\rm in}}}\ . \tag{14}$$

We would like this variance to be zero. If both signal and probe inputs are in vacuum or coherent states with unit quantum variance in both quadratures, then

$$V_{X_a^{\rm in}}=V_{Y_p^{\rm in}}=1\ ,$$
$$C^2_{X_a^{\rm in}Y_p^{\rm out}}=\eta^2\ ,$$
$$C^2_{X_a^{\rm in}X_a^{\rm out}}=1-\eta^2\ , \tag{15}$$
$$C^2_{X_a^{\rm out}Y_p^{\rm out}}=0\ ,$$
$$V(X_a^{\rm out}|Y_p^{\rm out})=1\ .$$

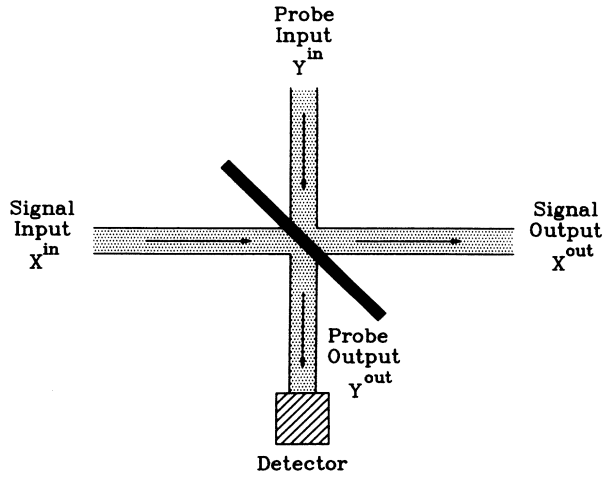


FIG. 3. A QND measurement scheme using a beam splitter.

As expected, the correlation between the signal input field and the signal output field is the intensity transmission coefficient for the mirror. To reduce the amount of noise added to the signal variable we would like to split off only a small portion of the light field. However, this reduces the correlation between the signal input field and the probe field upon which the readout measurement is made, which is given by the intensity reflection coefficient. It is not possible therefore to simultaneously satisfy the first two criteria for a good QND measurement scheme. Since the signal and probe output fields are completely uncorrelated, a measurement of the probe does not reduce the variance in the signal output variable at all. The result is that you cannot use a beam splitter to prepare the state of the output signal without the presence of a squeezing device. In Sec. VI we shall demonstrate how these conclusions are modified if a squeezed probe input is used.

## IV. QND MEASUREMENTS USING A RAMAN TRANSITION

The interaction between two light fields in a Raman transition creates a possible system for making QND measurements. We consider an arrangement in which we place a Raman-active medium inside an optical cavity, as illustrated in Fig. 4. If we label the intracavity mode corresponding to the external signal field as $a$, the corresponding mode for the probe as $b$, and the phonon mode as $c$, then the Raman interaction can be depicted as in Fig. 5. In Raman scattering, an incident photon energy $\hbar\omega_a$ is destroyed within the medium, while at the same time a second photon of energy $\hbar\omega_b$ is emitted. The difference between the two appears as a quantum of excitation in a vibrational mode of the medium itself, with energy $\hbar\omega_c$. Both spontaneous Raman scattering and stimulated Raman gain have this overall form. The many various Raman interactions have been reviewed in the context of coherent Raman spectroscopy.[9]

The appropriate Hamiltonian to describe this interaction is

$$H = i\hbar(\chi a^{\dagger} bc - \chi^* a b^{\dagger} c^{\dagger}) . \tag{16}$$

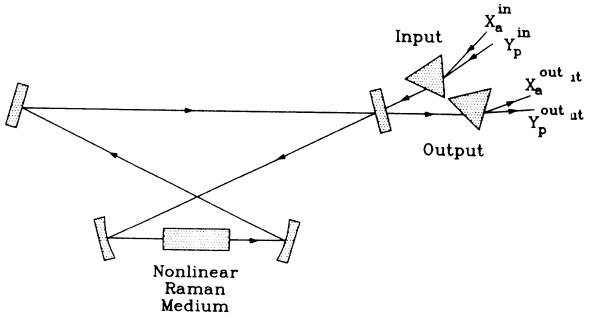


FIG. 4. A ring cavity containing a nonlinear Raman medium. The Raman transition produces coupling between the signal and probe fields allowing QND fluctuation measurements to be made.

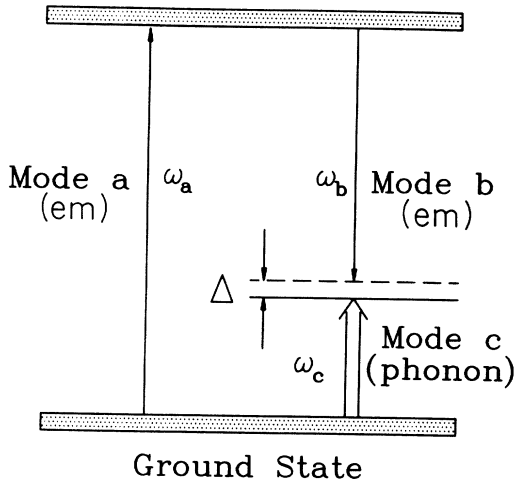


FIG. 5. The Raman transition. A photon at frequency $\omega_a$ is destroyed within the medium producing a photon at frequency $\omega_b$ and a Raman phonon exciting a vibrational mode of the medium itself. There is a detuning $\Delta$ between the levels of the system interaction.

While the strongest interaction will occur if the energy of the phonon is exactly equal to the difference of the destroyed and emitted photons, stimulated Raman loss and scattering will degrade the quantum correlations between the signal and probe fields. We also introduce a detuning $\Delta$ between the energy levels of the system,

$$\omega_b = \omega_a - \omega_c - \Delta . \tag{17}$$

The higher we make the detuning, the weaker the nonlinearity becomes; however, the effects of stimulated loss and scattering are less. We wish to find the optimum conditions for a QND measurement. To solve this problem we proceed using standard quantum statistical techniques. The first step is to remove the high-frequency behavior of the system operators by transforming to the interaction picture:

$$\begin{aligned} a_i &= a e^{i\omega_a t} , \\ b_i &= b e^{i\omega_b t} , \\ c_i &= c e^{i(\omega_c + \Delta)t} . \end{aligned} \tag{18}$$

The Langevin equations of motion for this system are

$$\begin{aligned} \frac{da_i}{dt} &= \chi b_i c_i - \frac{\gamma_a}{2} a_i - \sqrt{\gamma_a}\, a_{\mathrm{in},i} , \\ \frac{db_i}{dt} &= -\chi^* a_i c_i^{\dagger} - \frac{\gamma_b}{2} b_i - \sqrt{\gamma_b}\, b_{\mathrm{in},i} , \\ \frac{dc_i}{dt} &= i\Delta c_i - \chi^* a_i b_i^{\dagger} - \frac{\gamma_c}{2} c_i - \sqrt{\gamma_c}\, c_{\mathrm{in},i} . \end{aligned} \tag{19}$$

Here $\gamma_a, \gamma_b$, and $\gamma_c$ are the cavity line widths for the three modes, and the Langevin noise sources $a_{\mathrm{in}}$ and $b_{\mathrm{in}}$ are the signal and probe inputs at the cavity mirror in the usual way, with $c_{\mathrm{in}}$ corresponding to phonon noise introduced from a thermal bath. Implicit in the choice of $\gamma_a$

and $\gamma_b$ real is the assumption that the cavity is simultaneously resonant at both optical frequencies. In a high-$Q$ optical cavity, the linewidth $\gamma_c$ for the phonon mode is very much larger than that for the two optical modes. This allows us to adiabatically eliminate the phonon mode by setting

$$\frac{dc_i}{dt} \approx 0 \ . \tag{20}$$

The equation of motion for the phonon operator can be solved, giving

$$c_i = -\frac{\chi^*}{\frac{\gamma_c}{2} - i\Delta} a_i b_i^\dagger - \frac{\sqrt{\gamma_c}}{\frac{\gamma_c}{2} - i\Delta} c_{\text{in},i} \ . \tag{21}$$

The phase of the phonon mode in this regime is thus given by the phase difference of the two optical modes with an additional detuning phase shift $\phi_d$, where

$$\tan\phi_d = 2\Delta_c \ . \tag{22}$$

Here $\Delta_c$ is the detuning measured in phonon linewidths

$$\Delta_c \equiv \frac{\Delta}{\gamma_c} \ . \tag{23}$$

Equations (19) can then be written as

$$\begin{aligned} \frac{da_i}{dt} &= -\frac{2\chi}{\gamma_c}(\cos\phi_d) e^{i\phi_d}(\chi^* a_i b_i^\dagger b_i + \sqrt{\gamma_c} b_i c_{\text{in},i}) \\ &\quad - \frac{\gamma_a}{2} a_i - \sqrt{\gamma_a} a_{\text{in},i} \ , \\ \frac{db_i}{dt} &= \frac{2\chi^*}{\gamma_c}(\cos\phi_d) e^{-i\phi_d}(\chi a_i^\dagger a_i b_i + \sqrt{\gamma_c} a_i c_{\text{in},i}^\dagger) \\ &\quad - \frac{\gamma_b}{2} b_i - \sqrt{\gamma_b} b_{\text{in},i} \ . \end{aligned} \tag{24}$$

These resulting equations are nonlinear, and hence in order to solve them we linearize about the steady-state amplitudes for each of the modes. In order to simplify the resulting equations we also transform to the *signal interaction picture,*

$$\begin{aligned} a_{\text{sg}} &= U^\dagger a_i U \\ b_{\text{sg}} &= U^\dagger b_i U \ , \end{aligned}$$

with the unitary operator

$$U = \exp\left[ i \frac{|\chi|^2}{\gamma_c} \sin(2\phi_d)(|\alpha|^2 b_i^\dagger b_i + |\beta|^2 a_i^\dagger a_i) t \right] . \tag{25}$$

Linearizing about the mean amplitudes $\alpha$ and $\beta$,

$$\begin{aligned} a_{\text{sg}} &= \alpha + a_f \ , \\ b_{\text{sg}} &= \beta + b_f \ , \end{aligned} \tag{26}$$

and defining scaled intensities for the signal and probe internal fields,

$$\begin{aligned} A &= \frac{4|\chi|^2}{\gamma_b \gamma_c (1+4\Delta_c^2)} |\alpha|^2 \ , \\ B &= \frac{4|\chi|^2}{\gamma_a \gamma_c (1+4\Delta_c^2)} |\beta|^2 \ , \end{aligned} \tag{27}$$

gives the following equations for the mean values:

$$\begin{aligned} \frac{\gamma_a}{2}\alpha(1+B) &= -\sqrt{\gamma_a}\alpha_{\text{in}} \ , \\ \frac{\gamma_b}{2}\beta(1-A) &= -\sqrt{\gamma_b}\beta_{\text{in}} \ . \end{aligned} \tag{28}$$

Here we have set $\langle \beta c_{\text{in,sg}} \rangle$ and $\langle \alpha c_{\text{in,sg}}^\dagger \rangle$ to zero, which is only valid if the number of thermally introduced phonons is small. Using the usual boundary conditions at the mirror surface,

$$\begin{aligned} \alpha_{\text{out}} &= \alpha_{\text{in}} + \sqrt{\gamma_a}\alpha \ , \\ \beta_{\text{out}} &= \beta_{\text{in}} + \sqrt{\gamma_b}\beta \ , \end{aligned} \tag{29}$$

the mean fields leaving the cavity can be related to the incident fields,

$$\begin{aligned} \alpha_{\text{out}} &= -\frac{1-B}{1+B}\alpha_{\text{in}} \ , \\ \beta_{\text{out}} &= -\frac{1+A}{1-A}\beta_{\text{in}} \ . \end{aligned} \tag{30}$$

It can be seen from this result that the interaction does not cause any phase shift in the output optical fields. Implicit in this is again the assumption that both modes are exactly on resonance with the cavity or else even in the absence of the nonlinear interaction the cavity will cause a phase shift. The parameter $A$ can be defined as the in-

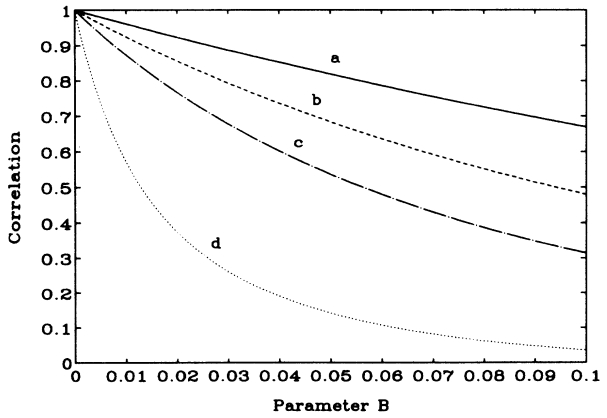


FIG. 6. $C^2_{X_a^{\text{in}} X_a^{\text{out}}}$ as a function of the probe intracavity intensity for curve $a$, $A=0$; $b$, $A=0.1$; $c$, $A=0.2$; and $d$, $A=0.5$.

tracavity intensity of the signal scaled so that at $A=1$, the intensity of the signal is sufficiently strong to cause free oscillations in the cavity amplifying spontaneous emission at the probe frequency. Similarly, the parameter $B$ can be defined as the intracavity intensity of the probe scaled so that at $B=1$, the probe is sufficiently intense to completely deplete the signal field leaving the apparatus. No matter what the probe detuning $\Delta_c$, stimulated Raman oscillation starting from vacuum fluctuations will occur at $\omega_s=\omega_a-\omega_c$ whenever the intracavity signal field exceeds $|\alpha|^2_{\max}=\gamma_c/(4|\chi|^2)\gamma_s$, where $\gamma_s$ is the cavity loss at $\omega_s$. A similar phenomenon limits the maximum probe field to $|\beta|^2_{\max}=\gamma_c/(4|\chi|^2)\gamma_{ss}$, where the second Stokes frequency is $\omega_{ss}=\omega_b-\omega_c$ and the cavity mode nearest $\omega_{ss}$ has width $\gamma_{ss}$. A tuning element may be included in the cavity to suppress these oscillations by making $\gamma_s \gg \gamma_b$ and also $\gamma_{ss} \gg \gamma_a$.

If we now make $\chi$, $\alpha$, and $\beta$ real, then the equations of motion for the fluctuation operators are

$$\begin{aligned}
\frac{da_f}{dt} &= -\frac{\gamma_a}{2}(1+B)a_f \\
&\quad -\frac{2\chi\beta}{\gamma_c}(\cos\phi_d)e^{i\phi_d}(\chi\alpha Y_a+\sqrt{\gamma_c}c_{\text{in},f}) \\
&\quad -\sqrt{\gamma_a}a_{\text{in},f}\ , \\
\frac{db_f}{dt} &= -\frac{\gamma_b}{2}(1-A)b_f \\
&\quad +\frac{2\chi\alpha}{\gamma_c}(\cos\phi_d)e^{-i\phi_d}(\chi\beta X_a+\sqrt{\gamma_c}c^\dagger_{\text{in},f}) \\
&\quad -\sqrt{\gamma_b}b_{\text{in},f}\ ,
\end{aligned} \tag{31}$$

where $X_a$ and $Y_a$ are the signal and probe amplitude fluctuation quadratures, $X_p$ and $Y_p$ are the corresponding phase fluctuation operators, and all the relevant quadratures for the fluctuation operators of the external and internal fields are defined by

$$\begin{aligned}
&X_a=a_f+a_f^\dagger,\quad X_p=i(a_f^\dagger-a_f)\ , \\
&Y_a=b_f+b_f^\dagger,\quad Y_p=i(b_f^\dagger-b_f)\ , \\
&X_a^{\text{in}}=a_{\text{in},f}+a_{\text{in},f}^\dagger,\quad X_p^{\text{in}}=i(a_{\text{in},f}^\dagger-a_{\text{in},f})\ , \\
&Y_a^{\text{in}}=b_{\text{in},f}+b_{\text{in},f}^\dagger,\quad Y_p^{\text{in}}=i(b_{\text{in},f}^\dagger-b_{\text{in},f})\ , \\
&Z_a^{\text{in}}=c_{\text{in},f}e^{i\phi_d}+c_{\text{in},f}^\dagger e^{-i\phi_d}\ ,\quad Z_p^{\text{in}}=i(c_{\text{in},f}^\dagger e^{-i\phi_d}-c_{\text{in},f}e^{i\phi_d})\ .
\end{aligned} \tag{32}$$

Using this, we can then derive four equations of motion for the intracavity quadratures by taking sums and differences of Eq. (31):

$$\frac{d}{dt}\begin{bmatrix}X_a\\X_p\\Y_a\\Y_p\end{bmatrix}=\begin{bmatrix}
-\frac{\gamma_a}{2}(1+B) & 0 & -\sqrt{\gamma_a\gamma_b AB} & 0 \\
0 & -\frac{\gamma_a}{2}(1+B) & -2\Delta_c\sqrt{\gamma_a\gamma_b AB} & 0 \\
\sqrt{\gamma_a\gamma_b AB} & 0 & -\frac{\gamma_b}{2}(1-A) & 0 \\
-2\Delta_c\sqrt{\gamma_a\gamma_b AB} & 0 & 0 & -\frac{\gamma_b}{2}(1-A)
\end{bmatrix}\begin{bmatrix}X_a\\X_p\\Y_a\\Y_p\end{bmatrix}+\begin{bmatrix}
-\sqrt{\gamma_a B}\,Z_a^{\text{in}}-\sqrt{\gamma_a}X_a^{\text{in}} \\
-\sqrt{\gamma_a B}\,Z_p^{\text{in}}-\sqrt{\gamma_a}X_p^{\text{in}} \\
+\sqrt{\gamma_b A}\,Z_a^{\text{in}}-\sqrt{\gamma_b}Y_a^{\text{in}} \\
-\sqrt{\gamma_b A}\,Z_p^{\text{in}}-\sqrt{\gamma_b}Y_p^{\text{in}}
\end{bmatrix}. \tag{33}$$

We solve these equations for $\omega=0$ by setting the left-hand side equal to zero. The problem then reduces to that of inverting the $4\times4$ matrix. This can be done using the following identity:

$$\begin{bmatrix}a&0&b&0\\0&a&c&0\\-b&0&d&0\\c&0&0&d\end{bmatrix}^{-1}=\frac{1}{ad(ad+b^2)}\begin{bmatrix}ad^2&0&-abd&0\\-bcd&ad^2+b^2d&-acd&0\\abd&0&a^2d&0\\-acd&0&abc&a^2d+ab^2\end{bmatrix}. \tag{34}$$

To eliminate the intracavity mode operators we apply appropriate boundary conditions at the mirror surfaces. These are

$$
\begin{aligned}
X_a^{\text{out}} &= X_a^{\text{in}} + \sqrt{\gamma_a} X_a \ , \\
X_p^{\text{out}} &= X_p^{\text{in}} + \sqrt{\gamma_a} X_p \ , \\
Y_a^{\text{out}} &= Y_a^{\text{in}} + \sqrt{\gamma_b} Y_a \ , \\
Y_p^{\text{out}} &= Y_p^{\text{in}} + \sqrt{\gamma_b} Y_p \ .
\end{aligned} \tag{35}
$$

This gives the following solutions for the output field amplitude quadratures:

$$
\begin{aligned}
X_a^{\text{out}} &= \frac{1}{D}\{[D-2(1-A)]X_a^{\text{in}} + 4\sqrt{AB}\, Y_a^{\text{in}} - 2\sqrt{B}\,(1+A)Z_a^{\text{in}}\} \ , \\
Y_a^{\text{out}} &= \frac{1}{D}\{[D-2(1+B)]Y_a^{\text{in}} - 4\sqrt{AB}\, X_a^{\text{in}} + 2\sqrt{A}\,(1-B)Z_a^{\text{in}}\} \ ,
\end{aligned} \tag{36}
$$

and for the phase quadratures,

$$
\begin{aligned}
X_p^{\text{out}} &= \frac{1}{D}\left[8\Delta_c\sqrt{AB}\, Y_a^{\text{in}} + \frac{16\Delta_c AB}{1+B}X_a^{\text{in}} - D\frac{1-B}{1+B}X_p^{\text{in}} - 8\Delta_c A\sqrt{B}\,\frac{1-B}{1+B}Z_a^{\text{in}} - \frac{2D\sqrt{B}}{1+B}Z_p^{\text{in}}\right] \ , \\
Y_p^{\text{out}} &= \frac{1}{D}\left[8\Delta_c\sqrt{AB}\, X_a^{\text{in}} - \frac{16\Delta_c AB}{1-A}Y_a^{\text{in}} - D\frac{1+A}{1-A}Y_p^{\text{in}} + 8\Delta_c B\sqrt{A}\,\frac{1+A}{1-A}Z_a^{\text{in}} - \frac{2D\sqrt{A}}{1-A}Z_p^{\text{in}}\right] \ ,
\end{aligned} \tag{37}
$$

where $D$ is defined as

$$
D \equiv (1+B)(1-A)+4AB \ . \tag{38}
$$

## V. EVALUATION OF THE RAMAN SCHEME

We can now establish how well the near-resonant Raman transition will perform as a quantum nondemolition measurement scheme using the criteria previously outlined.

### A. Signal degradation in the cavity

If we assume unit quantum noise from both the phonon bath and from the optical sources, then the correlation between the signal input field and the signal output field is given by

$$
C^2_{X_a^{\text{out}} X_a^{\text{in}}} = \frac{[D-2(1-A)]^2}{[D-2(1-A)]^2 + 16AB + 4B(1+A)^2} \ . \tag{39}
$$

A graph of this function is given in Fig. 6. The input-output correlation of the signal quadrature is large only near $A=B=0$. The maximum value of unity is achieved only at $B=0$ as stimulated Raman loss interactions otherwise add noise. Even without loss, the sort of device proposed here unacceptably degrades the signal quadrature fluctuations when the normalized intracavity powers are larger than roughly 0.1.

### B. Optimum measurement correlations

The appropriate quantity to consider here is the correlation coefficient between the amplitude quadrature of the input signal and the phase quadrature of the probe output field. Once again assuming unit quantum noise from all sources, this can be written

$$
C^2_{X_a^{\text{in}} Y_p^{\text{out}}} = \frac{64\Delta_c^2 AB(1-A)^2}{64\Delta_c^2 AB[(1-A)^2 + 4AB + B(1+A)^2] + D^2[4A + (1+A)^2]} \ . \tag{40}
$$

An illustration of dependence of this function on the intracavity field intensities is given in Fig. 7 for a detuning of $\Delta_c = 4$. The optimum operating point around $A=0.11$ and $B=0.08$ achieves a correlation of $C^2_{X_a^{\text{in}} Y_p^{\text{out}}} = 0.71$. Figure 8 illustrates this optimum correlation for detunings of 0–10 photon linewidths away from the Raman resonance, showing how stimulated Raman loss and scattering destroys the measurement correlation when the detuning is too small. Figure 9 shows the normalized intracavity power that results in this optimum. The maximum correlation appears always to occur near $A=0.1$ for all detunings. The value of $B$ that gives the best correlation decreases as $\Delta_c$ increases, but the necessary power to achieve the best correlation increases with detuning. For detunings less than 2, the maximum correlation is predicted to be less than 0.52. The actual power

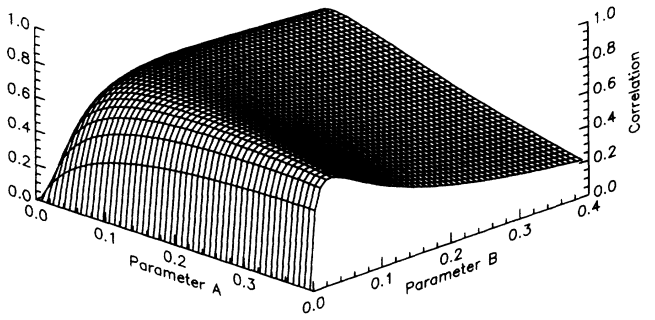


FIG. 7. An illustration of $C^2_{X_a^{\rm in}Y_p^{\rm out}}$, the correlation of the signal input field to the probe output field, as a function of the signal and probe intracavity intensities for $\Delta_c=4$. The maximum of 0.71 lies at $A=0.11$ and $B=0.08$.

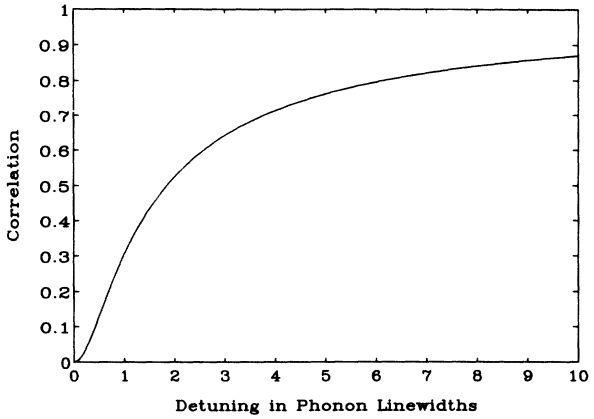


FIG. 8. The maximum possible $C^2_{X_a^{\rm in}Y_p^{\rm out}}$ for a given detuning.

needed to achieve this correlation is more modest than for larger detunings where the Raman nonlinearity is reduced. For $\Delta_c=10$, the maximum correlation is nearly 90%, and near optimum correlation occurs over a wide range of power.

A good QND device, however, must not only make a good measurement but must also not degrade the signal field significantly in the region of operation. We consider then simultaneously maximizing both correlation coefficients by considering their equally weighted sum

$$\frac{1}{2}(C^2_{X_a^{\rm in}X_a^{\rm out}}+C^2_{X_a^{\rm in}Y_p^{\rm out}}) .$$

For the beam splitter this equals $\frac{1}{2}$ and is independent of the mirror reflectivity. Figure 10 illustrates this for the Raman cavity, showing the dependence of the sum on the detuning. The intracavity signal and probe internal fields have been chosen to maximize the sum. For detunings less than $\Delta_c=1.5$, the optimum operating point is for the cavity to reflect all of the signal field and not to make a measurement at all. However, for detunings greater than this, it is possible to improve significantly on the beam splitter. For example, with $\Delta_c=4$, and a signal input to signal output correlation of 0.8, it is possible to obtain a measurement correlation of 0.61. In comparison, a beam splitter with the same signal degradation could record only a measurement correlation of 0.2.

### C. The Raman scheme as a state-preparation device

To measure how well we can predict the state of the signal field leaving the cavity, we are required to calculate the degree of variance in the signal output field given that a particular value for the probe has been recorded. The probe output field to signal output field correlation and the variance in the signal output field can be written as

$$C^2_{X_a^{\rm out}Y_p^{\rm out}}=\frac{64\Delta_c^2AB\{(1-A)[D-2(1-A)]-8AB-2B(1+A)^2\}^2}{\{[D-2(1-A)]^2+16AB+4B(1+A)^2\}\{64\Delta_c^2AB[(1-A)^2+4AB+B(1+A)^2]+D^2[4A+(1+A)^2]\}} ,$$

$$V(X_a^{\rm out})=\frac{1}{D^2}\{[D-2(1-A)]^2+16AB+4B(1+A)^2\} . \tag{41}$$

The residual variance after the measurement can then be determined using Eq. (9). Figure 11 is an illustration of this function for $\Delta_c=4$. A minimum variance of 0.31 is achieved for normalized intracavity powers of $A=B=0.09$. Figure 12 shows the dependence of the residual variance on the interaction detuning with Fig. 13 indicating the intracavity power which results in this minimum variance. Again the loss and scattering at low detunings destroys the QND nature of the scheme. For optimum state preparation, the required normalized probe power drops with increased detuning, while the normalized signal power increases. In absolute power units, reaching optimum as a state preparation device requires more power the larger the detuning for both probe and signal.

### D. The optimum probe phase

At infinite detuning from the Raman line center, the coupling is between the amplitude quadrature of the signal and the phase quadrature of the probe as previously stated. However, for the finite detuning considered here, the optimum quadrature phase may include some of the probe amplitude as well. Let the best quadrature phase be denoted by

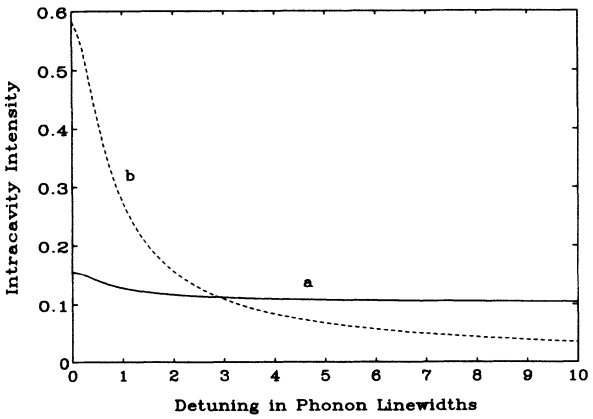


FIG. 9. Values of the intracavity fields which result in the maximum possible measurement correlation. The two graphs illustrated are curve $a$, the normalized signal field $A$, and $b$, the normalized probe field $B$.

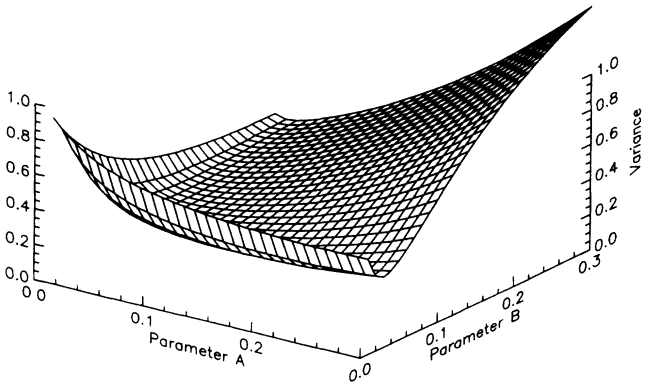


FIG. 11. An illustration of $V(X_a^{\text{out}}/Y_p^{\text{out}})$, the variance in the signal output field after a measurement of the probe, for $\Delta_c=4$. This is a measure of how well the scheme acts as a state preparation device. The minimum of 0.31 lies at $A=B=0.09$.

$$
\begin{aligned}
Y_b^{\text{out}} &= e^{-i\epsilon}b^{\text{out}}+e^{i\epsilon}b^{\text{out}\dagger} \\
&= (\cos\epsilon)(b^{\text{out}}+b^{\text{out}\dagger}) \\
&\quad -i(\sin\epsilon)(b^{\text{out}}-b^{\text{out}\dagger}) \\
&= (\cos\epsilon)Y_a^{\text{out}}+(\sin\epsilon)Y_p^{\text{out}} \ . \qquad (42)
\end{aligned}
$$

Using Eqs. (37), this gives

$$
Y_b^{\text{out}}=\frac{1}{D}[T_1X_a^{\text{in}}+T_2Y_a^{\text{in}}+T_3Y_p^{\text{in}}+T_4Z_a^{\text{in}}+T_5Z_p^{\text{in}}] \ , \qquad (43)
$$

where

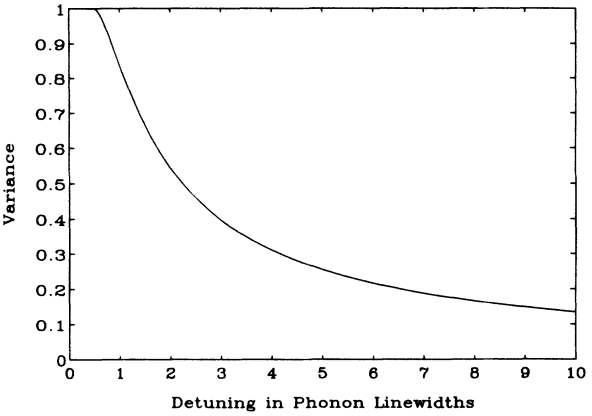


FIG. 12. The minimum possible $V(X_a^{\text{out}}|Y_p^{\text{out}})$ for a given detuning.

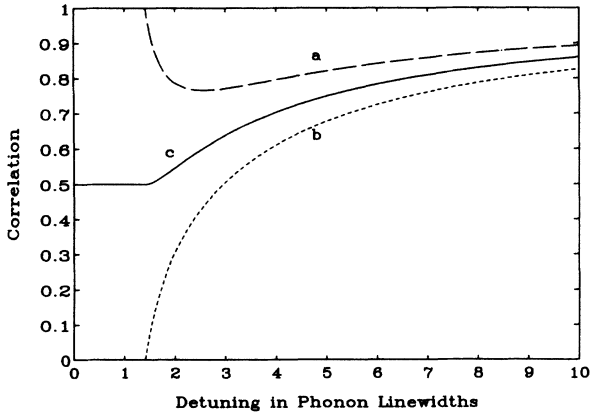


FIG. 10. The normalized signal and probe internal fields $A$ and $B$ chosen to maximize $\frac{1}{2}(C^2_{X_a^{\text{in}}X_a^{\text{out}}}+C^2_{X_a^{\text{in}}Y_p^{\text{out}}})$. Illustrated is curve $a$, $C^2_{X_a^{\text{in}}X_a^{\text{out}}}$; $b$, $C^2_{X_a^{\text{in}}Y_p^{\text{out}}}$; and $c$, the equally weighted sum of the two correlations. The value for a comparative beam splitter is $\frac{1}{2}$ and is independent of the mirror reflectivity. Above detunings of 1.5 photon linewidths, the diagram illustrates that there are regimes in which the Raman cavity has an enhanced performance with respect to the beam splitter.

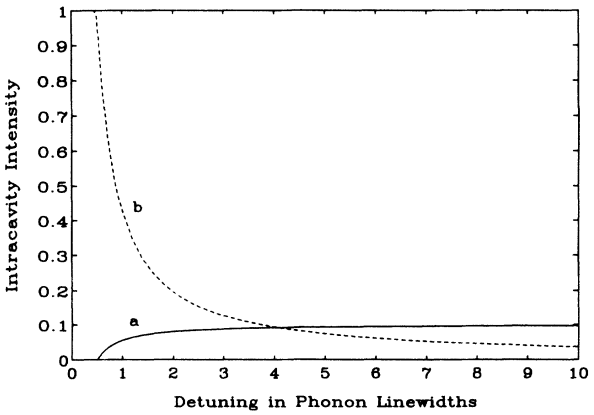


FIG. 13. Values of the intracavity fields which result in the minimum possible variance in the output signal. The two graphs illustrated are curve $a$, the normalized signal field $A$, and $b$, the normalized probe field $B$.

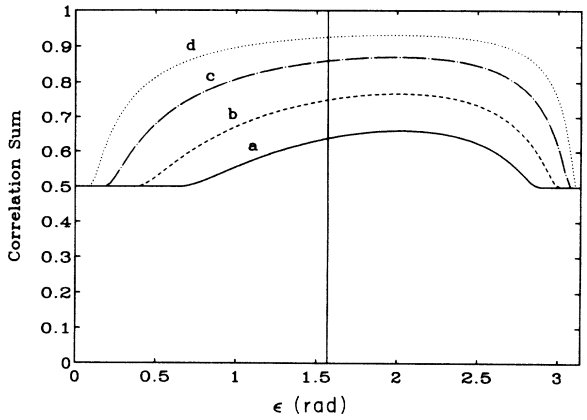


FIG. 14. Weighted sum of $C^2_{X_a^{\rm in}X_a^{\rm out}}$ and $C^2_{X_a^{\rm in}Y_b^{\rm out}}$, demonstrating the best quadrature phase for the probe. Illustrated is curve $a$, $\Delta_c=3$; $b$, $\Delta_c=5$; $c$, $\Delta_c=10$; and $d$, $\Delta_c=20$.

$$T_1=4\sqrt{AB}\,(1-A)(2\Delta_c\sin\epsilon-\cos\epsilon)\ ,$$

$$T_2=[D-2(1+B)](1-A)\cos\epsilon-16\Delta_c AB\sin\epsilon\ ,$$

$$T_3=-D(1+A)\sin\epsilon\ , \tag{44}$$

$$T_4=2\sqrt{A}\,[(1+B)(1-A)\cos\epsilon+4\Delta_c B(1+A)\sin\epsilon]\ ,$$

$$T_5=-2D\sqrt{A}\sin\epsilon\ .$$

Then the measurement correlation coefficient is given by

$$C^2_{X_a^{\rm in}Y_b^{\rm out}}=\frac{T_1^2}{T_1^2+T_2^2+T_3^2+T_4^2+T_5^2}\ . \tag{45}$$

To evaluate the optimum operating phase, we consider a system maximizing the sum

$$\tfrac{1}{2}(C^2_{X_a^{\rm in}X_a^{\rm out}}+C^2_{X_a^{\rm in}Y_b^{\rm out}})\ . \tag{46}$$

Figure 14 illustrates the value of this sum for given $\epsilon$ maximized over the possible intracavity intensities, for detunings of $\Delta_c=3$, $\Delta_c=5$, $\Delta_c=10$, and $\Delta_c=20$. For amplitude to phase coupling we would expect the maxima of the graphs to lie at $\epsilon=\pi/2$, as indicated by the vertical line. However, the position of the peak is skewed to higher values of $\epsilon$ than this. Amplitude quadrature to phase quadrature coupling is not the optimum situation for finite detuning, but the improvement made by choosing the best quadrature phase is not great. Notice also that for large detuning, there is a broad range of $\epsilon$ that gives good measurement correlation as well as low signal degradation.

## VI. BEAM SPLITTER WITH SQUEEZED PROBE

As another example we shall consider a beam splitter with a squeezed probe. Such a system has been discussed by Shapiro as a means of detecting a signal without any significant degradation of the signal. Its usefulness as a QND device has been discussed by Yurke. In this section we shall evaluate its suitability as a QND measuring scheme according to the criteria set out in Sec. III.

The correlation functions for a beam splitter were given in Eqs. (11), (12), and (14). If we take the probe input as a perfectly squeezed vacuum, then

$$C^2_{X_a^{\rm in}X_a^{\rm out}}=C^2_{X_a^{in}Y_p^{\rm out}}=C^2_{X_a^{\rm out}Y_p^{\rm out}}=1\ , \tag{47}$$

for which the variance in the output signal variable after measurement of the probe field is

$$V(X_a^{\rm out}|\,Y_p^{\rm out})=0\ . \tag{48}$$

This is exactly what is required for a ideal QND device. Under these circumstances the device acts as a perfect von Neumann measuring device which reports an eigenvalue and subsequently leaves the system in the corresponding eigenstate. It also has the potential to prepare an ideally squeezed coherent field by introducing a coherent light source to the signal port. Note that in this case, the output contains fluctuations transmitted by the mirror, but that since the same fluctuations can be measured at the homodyne detector, the output can be predicted with complete precision. It is only knowledge of the measurement that allows collapse of the output signal state.

The ideally squeezed vacuum, however, requires an infinite mean photon number so is an unrealistic limit. If we consider the incident signal field to have unit quantum fluctuations in the amplitude quadrature, then it remains to evaluate how well the device can perform for a given squeezing in the incident probe field. We consider here all three criteria presented in Sec. II to be equally important and maximize their equally weighted sum

$$C^2_{X_a^{\rm in}X_a^{\rm out}}+C^2_{X_a^{\rm in}Y_p^{\rm out}}-V(X_a^{\rm out}|\,Y_p^{\rm out})$$

by choosing the best reflectivity of the beam splitter. Figure 15 illustrates this optimum operating point as the squeezing level in the incident probe field is varied, and Fig. 16 shows the reflectivity used to achieve this. Clearly, the noise component in the projected output state is worse than that in the incident field, but the level of de-

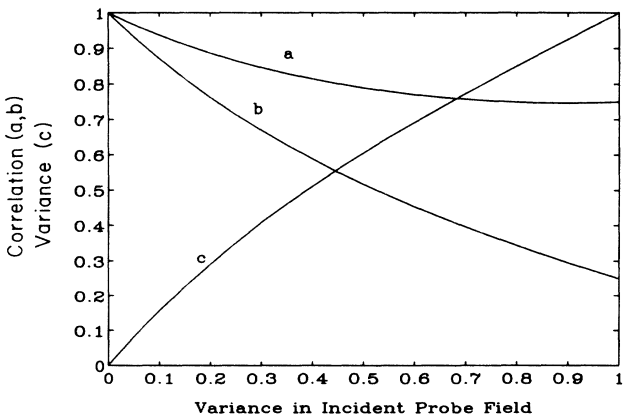


FIG. 15. The optimum operating point for a beam splitter as the level of squeezing in the probe field is varied. Shown is curve $a$, $C^2_{X_a^{\rm in}Y_p^{\rm out}}$; $b$, $C^2_{X_a^{\rm in}X_a^{\rm out}}$; and $c$, $V(X_a^{\rm out}|\,Y_p^{\rm out})$.

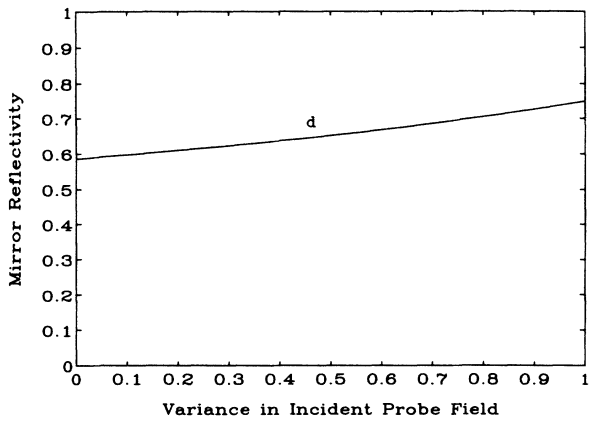


FIG. 16. The mirror reflectivity which gives the optimum operating point for making QND measurements using a beam splitter.

gradation is reasonably small. For a well-prepared probe incident field, with low noise variance in the phase quadrature, it is apparent that the scheme satisfies well the criteria outlined for a good QND measurement scheme.

## VII. CONCLUSION

We have developed in this paper a set of criteria for evaluating the effectiveness of quantum nondemolition measurement schemes in which an incident signal field couples strongly to a second probe field on which a subsequent readout measurement is made. This was used to firstly examine a beam splitter and then to evaluate a nonideal QND Hamiltonian corresponding to a near-resonance Raman transition. Phonon noise introduced from a thermal bath prevented the process from being ideally back action evading.

Significant signal degradation was found to occur if the intracavity intensity of either signal or probe was large. Optimum operating intensities were found for the measurement correlation, with reasonable results only for detunings further than two Raman linewidths off resonance. There are regimes of operation for detunings greater than $1\frac{1}{2}$ linewidths in which the Raman media has a significantly enhanced performance over a beam splitter. Unlike the beam splitter, the Raman cavity can also be used to partially prepare the state of the signal output field.

Even though it was not possible to find regimes of operation in which thermal noise could be completely isolated from the signal, interesting quantum correlations should be obtained at relatively large detunings from the Raman line center. We also demonstrated that a beam splitter with a squeezed probe can perform well as a QND measuring device under the criteria outlined in Sec. II.

## ACKNOWLEDGMENTS

We would like to thank Dr. S. M. Tan for helpful discussions and assistance in this paper. This research was supported by the New Zealand University Grants Committee and an IBM Joint Studies Agreement with the University of Auckland.

[1]C. M. Caves, K. S. Thorne, R. W. P. Drever, V. D. Sandberg, and M. Zimmerman, Rev. Mod. Phys. **52**, 341 (1980).
[2]G. J. Milburn and D. F. Walls, Phys. Rev. A **28**, 2055 (1983).
[3]N. Imoto, H. A. Haus, and Y. Yamamoto, Phys. Rev. A **32**, 2287 (1985).
[4]B. Yurke, J. Opt. Soc. Am. B **2**, 732 (1986).
[5]R. M. Shelby and M. D. Levenson Opt. Commun. **64**, 553 (1987).
[6]P. Alsing, G. J. Milburn, and D. F. Walls, Phys. Rev. A **37**, 2970 (1988).
[7]M. D. Levenson, R. M. Shelby, M. Reid, and D. F. Walls, Phys. Rev. Lett. **57**, 2473 (1986).
[8]A. La Porta, R. E. Slusher, and B. Yurke, Phys. Rev. Lett. **62**, 28 (1989).
[9]M. D. Levenson and S. S. Kano, *Introduction to Nonlinear Laser Spectroscopy* (Publisher, City, 1988).
[10]J. H. Shapiro, Opt. Lett. **5**, 351 (1980).
[11]B. Yurke (private communication).

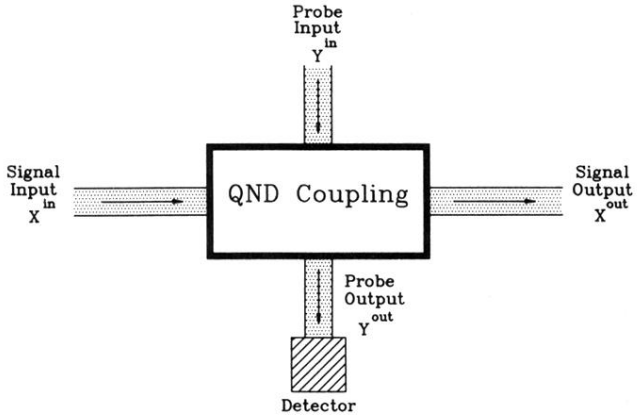


FIG. 1. A schematic quantum nondemolition device. The signal field interacts with the probe field in the apparatus. A subsequent readout measurement of the probe output is then well correlated with either the signal input making a good measurement, or the signal output preparing a well-known state.

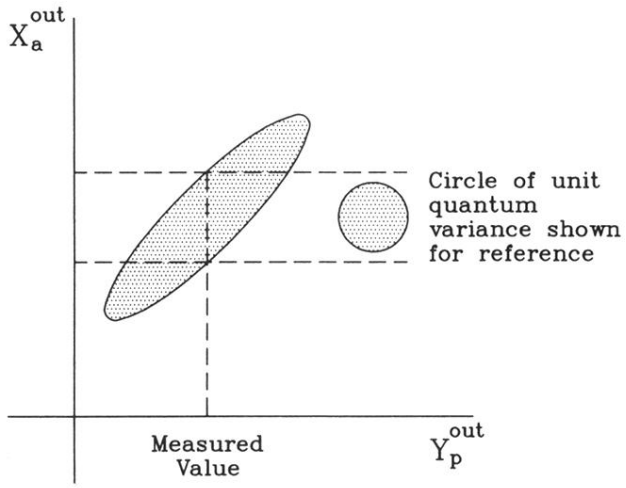


FIG. 2. Good correlation between the signal output and the probe output does not necessarily indicate a good state preparation device. The diagram illustrates a situation in which a value of the probe output has been measured but when mapped onto the error ellipse does not allow inference of the value of the signal to better than the quantum limit.

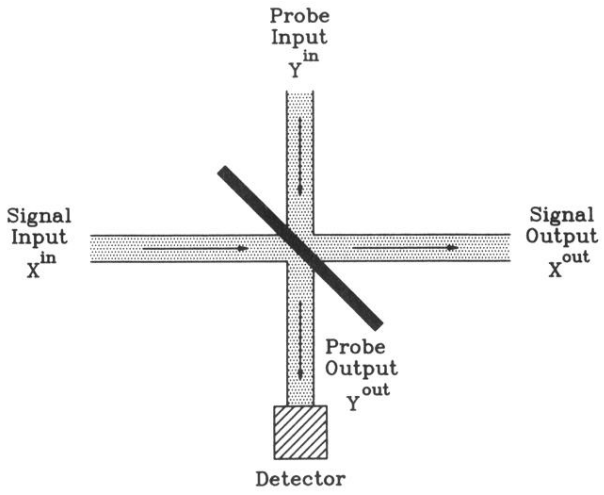


FIG. 3. A QND measurement scheme using a beam splitter.

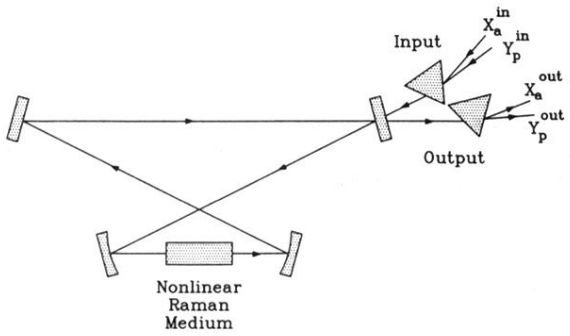


FIG. 4. A ring cavity containing a nonlinear Raman medium. The Raman transition produces coupling between the signal and probe fields allowing QND fluctuation measurements to be made.

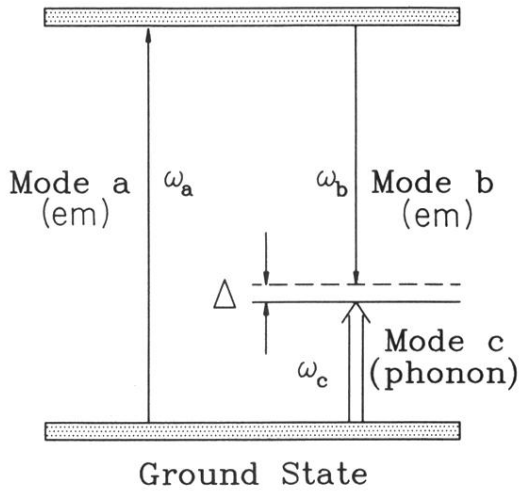


FIG. 5. The Raman transition. A photon at frequency $\omega_a$ is destroyed within the medium producing a photon at frequency $\omega_b$ and a Raman phonon exciting a vibrational mode of the medium itself. There is a detuning $\Delta$ between the levels of the system interaction.